Bioelectromagnetics 30:251–260 (2009)

Effect of Pulsed Electromagnetic Field on the Proliferation and Differentiation Potential of Human Bone Marrow Mesenchymal Stem Cells

Li-Yi Sun,[1,2] Dean-Kuo Hsieh,[3] Tzai-Chiu Yu,[4] Hsien-Tai Chiu,[2] Sheng-Fen Lu,[1] Geng-Hong Luo,[1] Tom K. Kuo,[5] Oscar K. Lee,[5,6] and Tzyy-Wen Chiou[1]***

[1]Department of Life Science and Graduate Institute of Biotechnology, National Dong Hwa University, Hualien, Taiwan, Republic of China
[2]Department of Biological Science and Technology, National Chiao Tung University, Hsinchu, Taiwan, Republic of China
[3]Department of Applied Chemistry, Chaoyang University of Technology, Taichung, Taiwan, Republic of China
[4]Department of Orthopaedics, Buddhist Tzu Chi General Hospital, Hualien, Taiwan, Republic of China
[5]Department of Orthopaedics and Traumatology, Taipei Veterans General Hospital, Taipei, Taiwan, Republic of China
[6]Institute of Clinical Medicine, National Yang-Ming University, Taipei, Taiwan, Republic of China

Pulsed electromagnetic fields (PEMFs) have been used clinically to slow down osteoporosis and accelerate the healing of bone fractures for many years. The aim of this study is to investigate the effect of PEMFs on the proliferation and differentiation potential of human bone marrow mesenchymal stem cells (BMMSC). PEMF stimulus was administered to BMMSCs for 8 h per day during culture period. The PEMF applied consisted of 4.5 ms bursts repeating at 15 Hz, and each burst contained 20 pulses. Results showed that about 59% and 40% more viable BMMSC cells were obtained in the PEMF-exposed cultures at 24 h after plating for the seeding density of 1000 and 3000 cells/cm^2, respectively. Although, based on the kinetic analysis, the growth rates of BMMSC during the exponential growth phase were not significantly affected, 20–60% higher cell densities were achieved during the exponentially expanding stage. Many newly divided cells appeared from 12 to 16 h after the PEMF treatment as revealed by the cell cycle analysis. These results suggest that PEMF exposure could enhance the BMMSC cell proliferation during the exponential phase and it possibly resulted from the shortening of the lag phase. In addition, according to the cytochemical and immunofluorescence analysis performed, the PEMF-exposed BMMSC showed multi-lineage differentiation potential similar to the control group. Bioelectromagnetics 30:251–260, 2009.

Key words: pulsed electromagnetic fields; human bone marrow; mesenchymal stem cells; growth kinetics; cell cycle; differentiation

INTRODUCTION

Pulsed electromagnetic fields (PEMFs) have been applied clinically to promote bone healing for many years [Heckman et al., 1981]. The clinical effectiveness was initially thought to be due to the accelerated formation of the bone matrix by the weak electric current generated by the magnetic field [Friedenberg and Brighton, 1966]. Studies have indicated that electromagnetic fields may heal bone fractures and slow down bone matrix loss in animal experiments [de Haas et al., 1980; Brighton et al., 1985a; McLeod and Rubin, 1992; Grace et al., 1998].

Despite the clinical success, electromagnetic fields have been reported to have negative effects on

*Correspondence to: Tzyy-Wen Chiou, Department of Life Science and Graduate Institute of Biotechnology, National Dong Hwa University, Hualien, No. 1, Sec. 2, Da Hsueh Rd., Shou-Feng, Hualien, Taiwan, Republic of China.
E-mail: twchiou@mail.ndhu.edu.tw

**Correspondence to: Oscar K. Lee, Institute of Clinical Medicine, National Yang-Ming University, Veterans General Hospital-Taipei, No. 201, Sec 2, Shi-Pai Road, Taipei 11221, Taiwan, Republic of China. E-mail: kslee@vghtpe.gov.tw

Received for review 29 December 2007; Final revision received 14 September 2008

DOI 10.1002/bem.20472
Published online 9 February 2009 in Wiley InterScience (www.interscience.wiley.com).

the proliferation and differentiation of bone cells [Norton, 1982; Norton et al., 1988]. Under specific electromagnetic fields, it has been observed that the proliferation of osteoblasts is limited and that alkaline phosphatase (ALP) activity is elevated [McLeod et al., 1993]. Recent research on the MG-63, ROS 17/2.8, and MLO-Y4 cell lines has shown that PEMF treatment either causes no effect or has a negative effect on cell proliferation [Sollazzo et al., 1997; Lohmann et al., 2000, 2003]. Furthermore, it was hard to explain the finding that PEMF stimulation significantly increased the proliferation of mouse osteoblasts, while the ALP staining and the mineralization remained the same [Chang et al., 2004b]. In another study, it was shown that treatment with PEMF alone or together with bone morphogenetic protein 2 (BMP-2) increased the cell proliferation and the differentiation of rat primary osteoblastic cells [Selvamurugan et al., 2007].

Current studies on stem cells have revealed that the regeneration of human body tissues and the supplement of mature functioning cells are due to the proliferation and differentiation of stem cells [Korbling and Estrov, 2003]. It was suggested that the proliferation and differentiation of human bone marrow mesenchymal stem cells (BMMSC) may lead to the replenishment of bone cells [Beresford, 1989; Pittenger et al., 1999; Halleux et al., 2001]. The mechanism of action underlying how PEMF promotes the formation of bone in an in vitro environment remains elusive. Therefore, we aim to investigate the influence of PEMF on the proliferation and differentiation potential of human BMMSC.

MATERIALS AND METHODS

Antibodies

Antibodies against human CD105 were purchased from Santa Cruz Biotechnology (Santa Cruz, CA). Antibodies against human CD13, CD14, CD29, CD34, CD44, CD45, HLA-ABC, and tau were purchased from Dako (Carpinteria, CA). Antibodies against human antigens CD73, CD90, HLA-DR, and microtubule-associated protein-2 (MAP2) were purchased from Becton Dickinson (Franklin Lakes, NJ). Antibodies against human antigens SH-2, SH-3, and SH-4 were purified from SH-2, SH-3, and SH-4 hybridoma cell lines (American Type Culture Collection, Rockville, MD). Secondary goat anti-mouse or anti-rabbit antibodies were from Chemicon (Temecula, CA).

BMMSC Isolation and Culture

The steps used for isolating human BMMSCs in this study were previously reported [Lee et al., 2004]. To maintain and expand the BMMSCs, the cells were cultured in expansion medium. Expansion medium consisted of Iscove's modified Dulbecco's medium (IMDM, Gibco, Grand Island, NY) and 10% fetal bovine serum (FBS, Hyclone, Logan, UT) supplemented with 10 ng/ml basic fibroblast growth factor (FGF-2, R&D Systems, Minneapolis, MN), 100 units penicillin, 1000 units streptomycin, and 2 mM L-glutamine. Once the cells reached 50–60% confluence, they were washed twice with phosphate-buffered saline (PBS), detached by 0.25% trypsin-EDTA (Gibco BRL) and then replated at a ratio of 1:4 under the same culture conditions. BMMSCs at passages 10–15 were used for the experiments in this study.

PEMF Exposure

The PEMF device (EBI, L. P., Parsippany, NJ) was placed in a CO_2 incubator (5% CO_2, 37 °C). For the PEMF treatment experiments, the BMMSCs were seeded at different densities in tissue culture flasks or six-well plates using expansion medium. Cultures were placed in the PEMF device (as shown in Fig. 1) and were exposed to PEMF 8 h per day during culture period. The applied field consisted of 4.5 ms bursts of 20 pulses repeating at 15 Hz [Bassett et al., 1974]. During each pulse, the magnetic field increased from 0 to 1.8 mT in 200 μs and then decayed back to 0 in 25 μs. Other signal parameters used in this study were described in detail by Guerkov et al. [2001] and

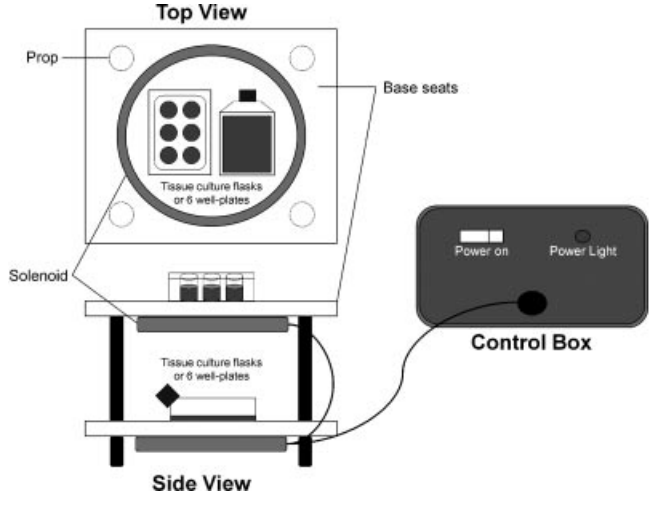

Fig. 1. Schematic representation of the pulsed electromagnetic fields device. The pulsed electromagnetic field device provided by EBI, L. P. was placed in a 5% CO_2 and 37 °C incubator. BMMSCs seeded in tissue culture flasks or six-well plates were placed on the base of the device for PEMF stimulation 8 h per day.

Lohmann et al. [2000, 2003]. The control experiments were performed on BMMSCs seeded in tissue culture flasks or six-well plates in a separate CO_2 incubator that had not been equipped with the PEMF device. The magnetic field inside the incubators did not differ from that present in the normal terrestrial field. The incubators were alternated for the treatment and control experiments.

Cell Growth Kinetics Analysis

As mentioned above, six-well plates seeded with BMMSCs in expansion medium with two different seeding cell densities (1000 and 3000 cells/cm^2) were placed in a CO_2 incubator in the presence or absence of PEMF stimulation. To follow the growth kinetics, cells were detached by trypsin-EDTA and a cell scraper (Becton Dickinson) and then counted by a hemocytometer under a microscope. The growth rate, which is the reciprocal of generation time, is defined as the number of cell doublings per unit of time during the specified time interval. The calculation of growth rate is as follows, $\mu = (3.32[\log_{10} N_t - \log_{10} N_0])/t$, where μ, N_t, and N_0 are the growth rates, final and initial cell densities, respectively. In this study, the calculated maximal growth rate represents the growth rate of the exponential phase during the culture process. These experiments were performed in triplicate and repeated in batches. Statistical analyses were performed using Student's *t*-test.

Cell Cycle Analysis

For cell cycle analysis, 75 cm^2 tissue culture flasks (Becton Dickinson) seeded with BMMSCs in expansion medium with an initial density of 1000 cells/cm^2 were placed in a CO_2 incubator in the presence of PEMF stimulation as previously described. Every 6 h, flasks ($n = 3$) were taken out of the incubator to detach and harvest the cells for cell cycle analysis. The harvested cells were washed in PBS and then fixed in cold 70% ethanol for 30 min at 4 °C. Fixed cells were washed twice in PBS, and spun at 2000 rpm. The resulting cell pellet was treated with 50 µl Ribonuclease A (10 µg/ml, Sigma, St. Louis, MO) and 1 ml propidium iodide staining solution (50 µg/ml, Sigma) for 3 h at 4 °C. Samples were stored at 4 °C until analyzed by flow cytometry (Becton Dickinson). In the control experiments, the BMMSCs cultured under the same conditions but without PEMF exposure were used. Statistical analyses were performed using Student's *t*-test.

Cell Surface Antigen Analysis

For the characterization of cell surface antigen phenotype, the BMMSCs were cultured in 75 cm^2 tissue culture flasks at an initial density of 1000 cells/cm^2 with expansion medium under regular PEMF treatment (i.e., 8 h a day) in a CO_2 incubator. After 3 or 8 days, cells were detached by trypsinization, stained with fluorescein isothiocyanate (FITC) or R-phycoerythrin (RPE) coupled antibodies, and then analyzed by flow cytometry (FACSCalibur, Becton Dickinson). In the control experiments, the BMMSCs were cultured under the same conditions but without PEMF treatment.

In Vitro Differentiation, Cytochemical and Immunofluorescence Analysis

BMMSCs at an initial density of 1000 cells/cm^2 were cultured under regular PEMF (8 h exposure each day) for 3 days and then redistributed into either 35 mm dishes or 25 cm^2 flasks at specified densities for the following in vitro differentiation experiments. BMMSCs cultured without PEMF were used in the control experiments. The following in vitro differentiations were performed with no PEMF exposure.

Osteogenic differentiation. BMMSCs after 3 days' PEMF treatment were seeded at a density of 5000 cells/cm^2 to study osteogenic differentiation. Cells were treated with osteogenic medium for 3 weeks; the medium was changed twice a week. Osteogenic medium consisted of high-glucose DMEM (Gibco BRL) and 10% FBS supplemented with 0.1 µM dexamethasone (Sigma), 10 mM β-glycerol phosphate (Sigma), 0.2 mM ascorbic acid (Sigma), 100 U penicillin, 1000 U streptomycin, and 2 mM L-glutamine. At weekly intervals, osteogenesis was evaluated by von Kossa staining and the activity of ALP.

von Kossa staining. The mineralized matrix of cells was assessed using 5% silver nitrate (Sigma) under ultra-violet light for 60 min, followed by 3% sodium thiosulphate (Sigma) for 5 min, and then counterstained with van Gieson (Sigma) for 5 min. The mineral was stained to black and osteoid was stained to red by this method.

Alkaline phosphatase staining. The ALP activity of cells was evaluated by an alkaline phosphatase histochemistry kit (Sigma #85). The reaction was performed for 60 min at 25 °C as recommended by the manufacturer. During incubation, culture dishes were protected from drying and light. Dishes were rinsed with deionized water, and air-dried prior to viewing.

Adipogenic differentiation. After 3 days' PEMF treatment, BMMSCs were seeded at a density of 5000 cells/cm^2 to induce adipogenic differentiation.

Cells were treated with adipogenic medium for 3 weeks. Adipogenic medium consisted of high-glucose DMEM supplemented with 0.5 mM 3-isobutyl-1-methylxanthine (IBMX, Sigma), 10 μg/ml insulin (Sigma), 1 μM dexamethasone, 0.1 mM indomethacin (Sigma), 100 U penicillin, 1000 U streptomycin, 2 mM L-glutamine, and 10% FBS. Medium changes were carried out twice a week and adipogenesis was assessed by oil red O staining at weekly intervals.

Oil red O staining. Adipogenic differentiation was demonstrated by the accumulation of lipid vesicles. Cells were fixed with 10% formalin, stained with oil red O (Sigma) for 10 min, and then counterstained with Mayer's hematoxylin (Sigma) for 1 min. The lipid vesicles were stained to red by this method.

Neurogenic differentiation. To induce neurogenic differentiation, a multi-step protocol was used. At a density of 10000 cells/cm^2, BMMSCs were seeded in 35 mm tissue culture dishes coated with 10 ng/ml fibronectin (Sigma). The cells were cultured with Step1 medium for 3 days, Step2 medium for 3 days, followed by Step3 medium for 1 day. Step1 medium consisted of IMDM, 20 ng/ml FGF-2, 20 ng/ml EGF (R&D), 10 ng/ml PDGF-BB (R&D), 0.5 μM retinoic acid (Sigma), 1 mM β-mercaptoethanol (Sigma), 100 U penicillin, 1000 U streptomycin, 2 mM L-glutamine, and ITS+ (Gibco BRL). Step2 medium consisted of IMDM supplemented with 20 ng/ml FGF-2, 20 ng/ml EGF, 10 ng/ml PDGF-BB, 0.5 μM RA, 100 U penicillin, 1000 U streptomycin, 2 mM L-glutamine, and ITS+. Step3 medium comprised NEUROBASAL Medium (Gibco BRL) supplemented with 10 ng/ml BDGF(R&D), 1 mM cAMP (Sigma), 0.5 mM IBMX, 200 μM BHA (Sigma), 100 μM ascorbic acid, N2 supplement (Gibco BRL), 100 U penicillin, 1000 U streptomycin, and 2 mM L-glutamine. Neurogenesis was assessed by immunofluorescence on day 7.

Immunofluorescence. For staining of intracellular proteins, cells on culture dishes were fixed for 10 min with 10% formalin at 25 °C, and permeabilized with 0.1% Triton X-100 (Sigma) for 5 min on ice. They were incubated with mouse primary antibodies against human MAP-2 (1:1000), and human tau (1:1000) for 1 h, followed by fluorescein-coupled goat anti-mouse or goat anti-rabbit IgG secondary antibody for 1 h. Between incubations, dishes were washed with PBS-T (0.1% tween-20, Sigma). Undifferentiated BMMSC cells were used as the negative control of immunofluorescence.

RESULTS

The Effect of PEMF Exposure on Growth Kinetics and Cell Cycle of BMMSCs

The growth kinetics of BMMSCs in the control and PEMF treatment experiments were monitored at two different cell seeding densities (1000 and 3000 cells/cm^2) as listed in Table 1. As examples, the semi-log plots of the growth curves for one batch of experimental results for each specific seeding density are shown in Figure 2A,B. The ratios of cell density of PEMF-exposed to non-exposed control during the first 4 days of the cell culture batch experiments for each seeding density are shown in Figure 3.

As indicated in Figure 2 and Table 1, the cell density of 24 h after plating showed significant difference between the control and PEMF groups. In the case of seeding density of 1000 cells/cm^2, the cell density increased from 1.00×10^3 cells/cm^2 to $1.18-1.23 \times 10^3$ in the control groups at day 1 after plating; however, it increased to $1.75-1.84 \times 10^3$ cell/cm^2 in the PEMF-treated groups at the same time, that is, about 59% more viable cells were obtained in the PEMF exposed culture at 24 h after plating (shown in Fig. 3A). Likewise, about 40% more viable cells were obtained in the PEMF-treated groups at 24 h after plating in the case of seeding density of 3000 cells/cm^2 (shown in Fig. 3B). It seems that the proliferation of the PEMF-treated BMMSC took off earlier than the untreated control group.

Moreover, as shown in Figure 2, the slopes during the exponential phase for the two seeding densities of the PEMF-treatment group and the non-treatment control group were quite similar. The calculated maximal growth rates in the exponential phase (as listed in Table 1) ranged from 5.59 to 5.88×10^{-2} h^{-1} and 5.39 to 5.81×10^{-2} h^{-1} for the batches at seeding density 1000 and 3000 cells/cm^2, respectively. No significant differences between the PEMF and control groups were shown among the batches for either seeding density. Although the growth rates in the exponential phase were comparable between the treatment and control groups, 20–60% higher cell densities were achieved in the PEMF group during the exponentially cell expanding stage, as shown in Figure 3. It is therefore suggested that the enhancement of cell proliferation by PEMF exposure might result from the shortening of lag phase.

In order to further investigate the effect of PEMF on cell growth, the cell cycle of propidium iodide stained BMMSCs in the control and experimental groups was analyzed by flow cytometry (Fig. 4A). Using total cell numbers as the basis, the proportion of the cells at various cell cycle stages was examined. As

TABLE 1. The Effect of PEMF Exposure on the Growth Kinetics of BMMSCs at Two Different Seeding Densities

	Cell density (10^3 cells/cm^2)								Maximal growth rate (10^{-2} h^{-1})	
	Day 1		Day 2		Day 3		Day 4			
Batch number	Control	PEMF	Control	PEMF	Control	PEMF	Control	PEMF	Control	PEMF
Seeding density 1000 cell/cm^2										
1	1.23 ± 0.09	$1.79 \pm 0.22^{\ddagger}$	3.19 ± 0.31	$4.53 \pm 0.47^{\ddagger}$	6.85 ± 0.20	$10.29 \pm 0.77^{\ddagger}$	17.03 ± 3.15	$23.80 \pm 2.48^{*}$	5.73 ± 0.14	5.58 ± 0.11
2	1.20 ± 0.14	$1.75 \pm 0.07^{*}$	3.15 ± 0.15	$4.40 \pm 0.28^{*}$	6.80 ± 0.14	$10.25 \pm 0.78^{*}$	14.30 ± 0.14	$21.70 \pm 0.42^{\dagger}$	5.80 ± 0.85	5.54 ± 0.63
3	1.18 ± 0.13	$1.84 \pm 0.23^{*}$	2.99 ± 0.14	$4.52 \pm 0.18^{\dagger}$	7.25 ± 0.49	$10.09 \pm 0.57^{\dagger}$	14.75 ± 0.50	$20.43 \pm 1.38^{\ddagger}$	5.59 ± 0.42	5.39 ± 0.12
4	1.21 ± 0.14	$1.80 \pm 0.12^{*}$	3.22 ± 0.31	$4.67 \pm 0.47^{\dagger}$	7.00 ± 0.47	$9.56 \pm 0.52^{*}$	15.18 ± 0.69	$21.88 \pm 1.81^{*}$	5.88 ± 0.42	5.73 ± 0.24
Seeding density 3000 cell/cm^2										
1	3.22 ± 0.62	$4.34 \pm 0.32^{*}$	5.11 ± 0.16	$7.34 \pm 0.32^{\dagger}$	10.65 ± 0.64	$14.80 \pm 0.71^{*}$	23.78 ± 5.34	$31.99 \pm 1.73^{*}$	5.71 ± 0.80	5.81 ± 0.02
2	3.49 ± 0.39	$4.57 \pm 0.16^{*}$	5.75 ± 0.40	$7.55 \pm 0.56^{*}$	10.88 ± 0.50	$13.64 \pm 0.32^{\dagger}$	27.89 ± 3.09	$34.12 \pm 2.65^{*}$	5.66 ± 0.91	5.51 ± 0.23
3	3.18 ± 0.56	$4.54 \pm 0.39^{*}$	5.55 ± 0.62	$8.00 \pm 0.11^{*}$	10.33 ± 0.32	$13.33 \pm 0.42^{*}$	26.28 ± 0.92	$34.15 \pm 0.64^{\dagger}$	5.61 ± 0.31	5.65 ± 0.63

$^{*}P < 0.05$.
$^{\dagger}P < 0.01$.
$^{\ddagger}P < 0.005$.

shown in Figure 4B, it is apparent that at the 6th hour (during the first PEMF exposure) and 12th hour (4 h after the first PEMF treatment), PEMF treatment led to a higher percentage of cells in the G2/M phase (representing DNA synthesis stage) by a difference of 3–4%. At the 18th hour (10 h after first PEMF treatment) and 24th hour (16 h after the first PEMF treatment), the percentage of cells at both the G2/M phase and S (DNA-synthesis) phase decreased by 8–12% and 3–4%, respectively; however, the proportion of cells at the G0/G1 phase (representing the newly divided cells) increased by 13–16%. At the 48th hour (16 h after the second PEMF exposure), the differences between the control and PEMF experiments were still significant, but the variations at this time were not as considerable as those in the 24th hour. These results imply that the first PEMF exposure affected the cell cycle and resulted in more newly divided cells than the control. The results support the findings obtained from the growth kinetics studies.

The Effect of PEMF Exposure on the Morphology and Immunophenotype of BMMSCs

As shown in Figure 5A, after human FGF-2 had been added to medium, the BMMSCs exhibited spindle-shape morphology [Martin et al., 1997; Halleux et al., 2001; Sottile et al., 2002; Bianchi et al., 2003]. No significant change in the morphology of the BMMSCs was observed after 3 days of PEMF treatment.

Analysis of the immunophenotype by flow cytometry showed that PEMF treatment for 3 or 8 days did not lead to significant changes in the surface phenotype of typical mesenchymal stem cells (Table 2).

Effect of PEMF Exposure on In Vitro Differentiation of BMMSCs

In order to determine whether the BMMSCs still have differentiation potential after PEMF treatment, in vitro osteogenic, adipogenic, and neurogenic differentiation experiments were conducted for both PEMF-treated and non-treated BMMSCs.

For osteogenic differentiation, BMMSCs at a density of 5000 cells/cm^2 were induced under osteogenic conditions. The mineralized matrix formed by the osteoblasts was confirmed by von Kossa staining (Fig. 5B), and positive staining for ALP (Fig. 5C). Both the PEMF-treated and non-PEMF treated BMMSCs possessed the potential for osteogenic differentiation.

To evaluate the adipogenic potential, BMMSCs with or without PEMF treatment at a density of

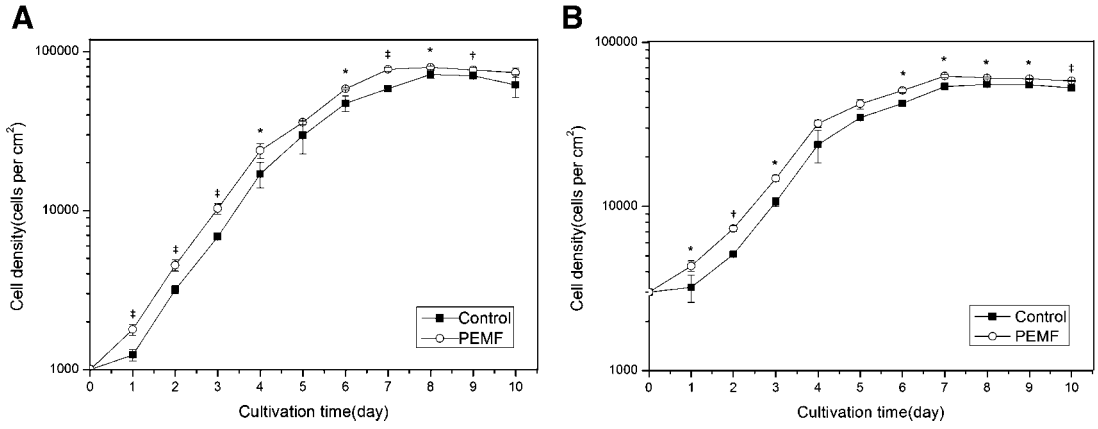

Fig. 2. The effect of PEMF exposure on the proliferation of BMMSCs at different seeding densities. **A**: Semi-log chart of cell growth at the seeding density of 1000 cells/cm^2. **B**: Semi-log chart of cell growth at the seeding density of 3000 cells/cm^2. The cell densities in the PEMF-exposed groups were significantly higher than those in the control group, especially during the exponential phase of cell culture experiments for both seeding densities tested. For both seeding densities, the maximal growth rates in the exponential phase were not significantly affected by PEMF treatment, as shown by the slope of the kinetic curves in the semi-log plots. The data points represent the mean cell number $\pm$ standard deviation ($n = 3$). $^*P < 0.05$. $^\dagger P < 0.01$. $^\ddagger P < 0.005$.

5000 cells/cm^2 were induced with adipogenic medium. After 3 days of induction, cells of both groups revealed adipogensis based on the apparent changes in cell morphology and the visible accumulation of neutral lipid vacuoles. At day 14, more than 80% of the cells showed neutral lipid vacuoles in the cells as confirmed by oil red O staining (Fig. 5D).

Using the multi-step neurogenic methods described earlier, both the PEMF-treated and non-treated BMMSCs showed neurite-like structures and convex-shaped cell bodies, indicating that they have the potential to differentiate into neuron-like cells (Fig. 4E). Immunofluoresence staining on the differentiated cells indicated the expression of neuron-related proteins, such as MAP2 (Fig. 5F) and tau (Fig. 5G).

DISCUSSION

PEMF therapy has been used successfully to cure a wide range of bone diseases for many years, including bone fractures [Grace et al., 1998] and osteoporosis [Brighton et al., 1985b,c; McLeod and Rubin, 1992]. However, the mechanism by which PEMF stimulation induces cellular proliferation and bone regeneration remains unclear. PEMF stimulation affects not only proliferation of osteoblasts, but also apoptosis of osteoclasts [Luben, 1991; McLeod et al., 1993; Chang et al., 2004a, 2006]. In addition, different characteristics of PEMF signals can reduce or enhance osteoclastogenesis of bone marrow cells [Chang et al., 2004a, 2005].

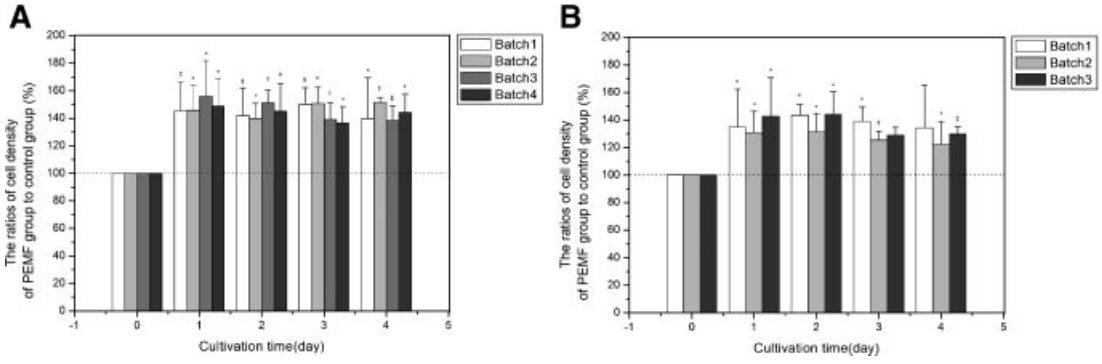

Fig. 3. Ratios of cell density of PEMF-exposed to non-exposed control during the first 4 days of the culture process. **A**: Batch results at seeding density of 1000 cells/cm^2. **B**: Batch results at seeding density of 3000 cells/cm^2. The results represent the mean cell number $\pm$ standard deviation ($n = 3$). $^*P < 0.05$. $^\dagger P < 0.01$. $^\ddagger P < 0.005$.

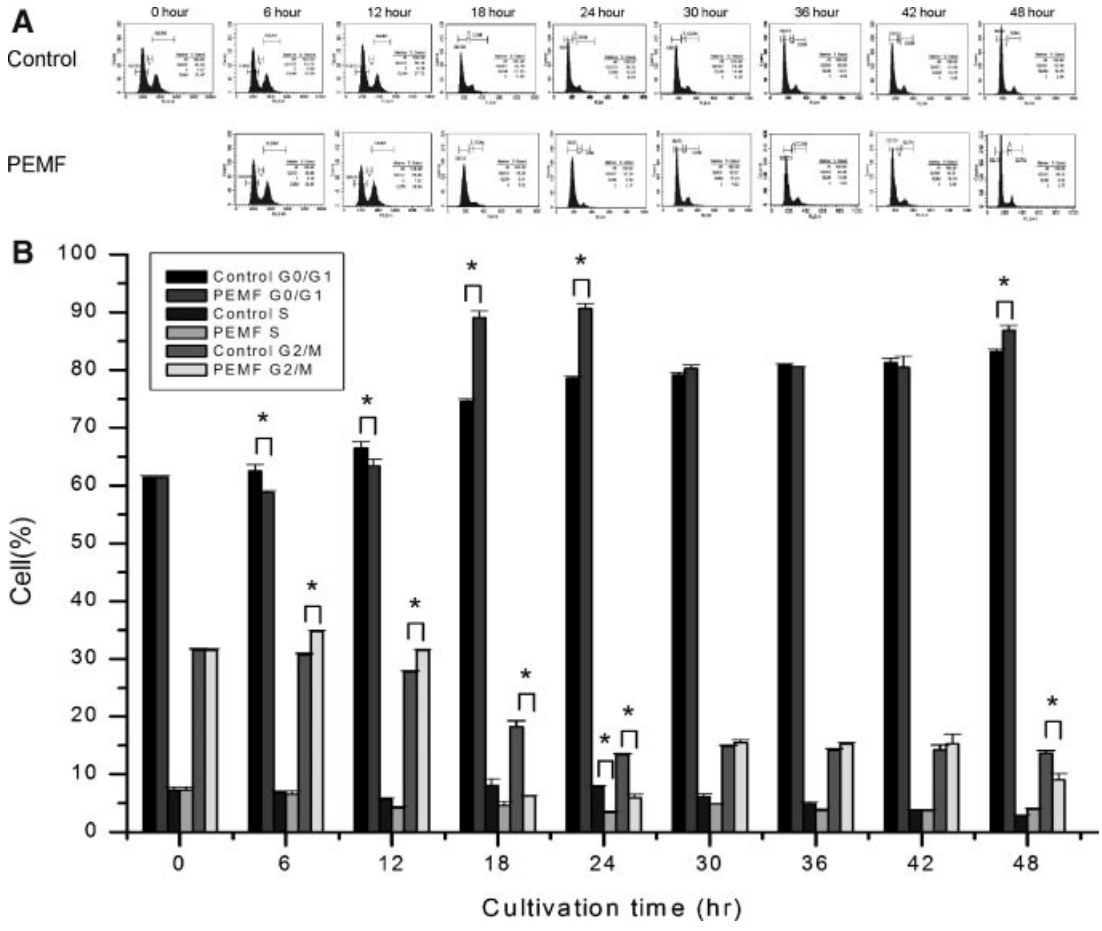

Fig. 4. The cell cycle of BMMSCs with or without PEMF exposure seeded at an initial density of 1000 cells/cm^2. **A**: The cell cycle of BMMSCs analyzed by propidium iodide staining and flow cytometry from 0 to 48 h. **B**: The percentages of cells in each phase of the cell cycle. At the 6th and 12th hours, PEMF treatment resulted in a 3–4% increase in the proportion of cells in the G2/M phase. At the 18th and 24th hours, the percentage of cells in the G2/M phase and S phase decreased by 8–12% and 3–4%, respectively; however, the proportion of cells in the G0/G1 phase increased by 13–16%. The results represent the mean percentage of cells ± standard deviation ($n = 3$). *$P < 0.05$.

However, bone regeneration requires the proliferation and differentiation of new osteoblasts from stem cells. The human bone marrow stromal system is believed to be the reservoir of stem cells [Civin et al., 1984; Owen and Friedenstein, 1988]. In particular, the BMMSC can repair a number of damaged tissues by the stimulation of mobilizing signals such as hypoxia, platelet-derived growth factor-AB (PDGF-AB) and insulin-like growth factor 1 (IGF-1) [Rochefort et al., 2006; Ponte et al., 2007]. Research has demonstrated the in vivo osteogenic potential [Goshima et al., 1991; Gundle et al., 1995; Quarto et al., 1995] and in vitro osteogenic differentiation of BMMSC [Pittenger et al., 1999].

There are quite a few studies analyzing the effects of PEMF stimulation on cell lines and on non-human osteoblasts in vitro [Lohmann et al., 2000, 2003; Diniz et al., 2002; Sakai et al., 2006; Selvamurugan et al., 2007]. Diniz et al. [2002] showed that PEMF treatment of osteoblasts in the early stages accelerated cellular proliferation, enhanced cellular differentiation, and increased bone tissue-like formation. Chang et al. [2004b] reported that PEMF stimulation significantly increased the proliferation of osteoblasts, but had no effect on the synthesis of extracellular matrix. In this study, we investigated the effect of PEMF on expanding BMMSCs in medium with human FGF-2. In the medium containing human FGF-2, the PEMF treatment led to the early take-off of cell proliferation and consequently resulted in higher cell densities during the exponentially growing phase (Fig. 2A,B). The enhancement of cell proliferation is shown in Figure 3. The achieved cell densities in PEMF group were 20–60% higher than those in the control group during the exponential growth phase.

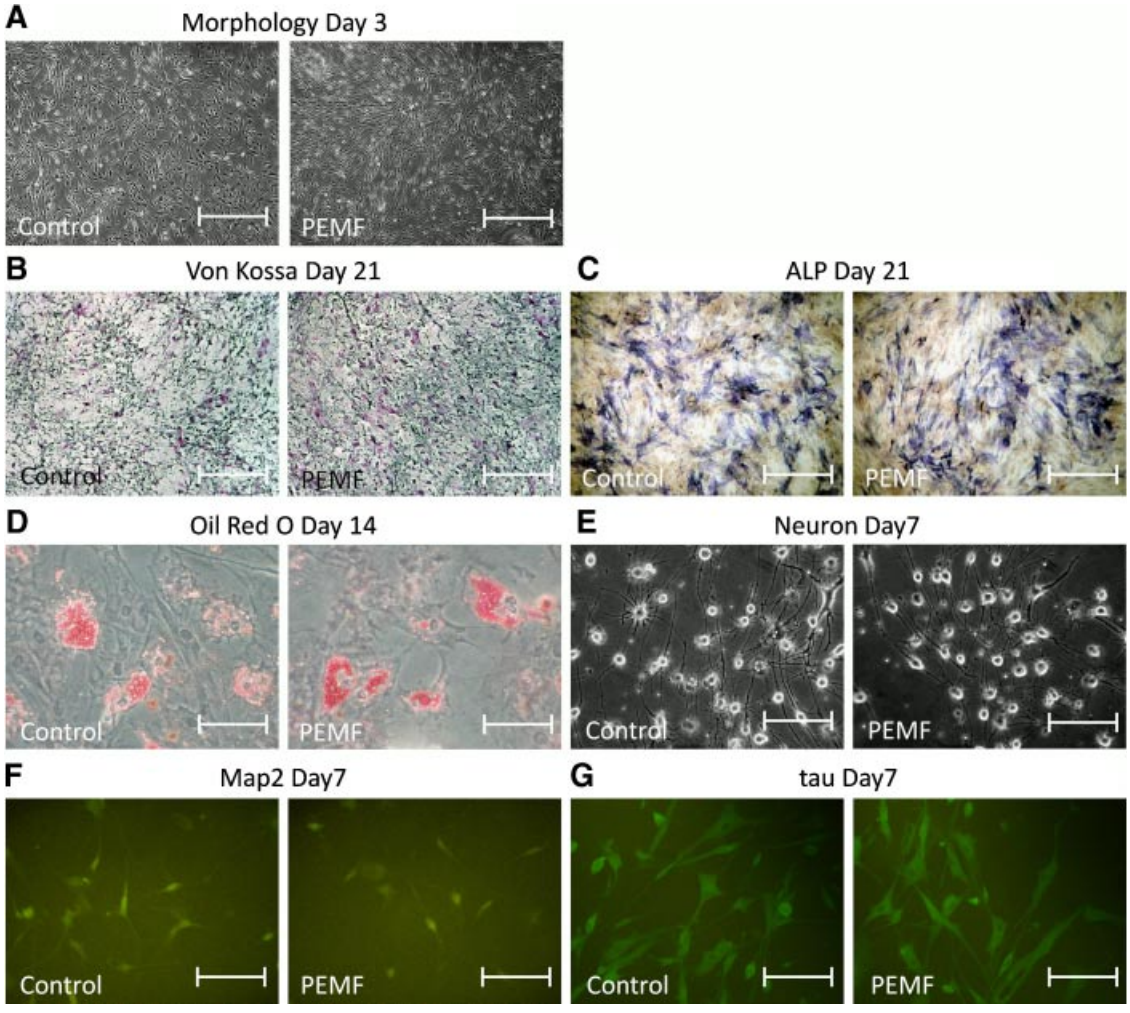

Fig. 5. PEMF had no effect on the morphology or differentiation potential of BMMSCs. **A**: morphology of BMMSCs at 3 days' culture with or without PEMF exposure. Cells possessed fibroblast-like morphology. Bar = 1 mm. To verify whether the BMMSCs still have differentiation potential after PEMF treatment, the differentiation experiments were conducted for both PEMF-treated and non-treated BMMSCs. Osteogenic differentiation after 14 days of induction was corroborated by formation of mineralized matrix as shown by (**B**) von Kossa staining and (**C**) ALP staining. Bar = 1 mm. Adipogenic differentiation was corroborated by (**D**) oil red O staining. Bar = 500 μm. Neurogenic differentiation was corroborated by (**E**) morphology after 7 days of induction, and by immunofluorescence assay for (**F**) MAP 2 and (**G**) tau. Bar = 500 μm. [The color figure for this article is available online at www.interscience.wiley.com.]

Minguell et al. [2001] and Conget and Minguell [1999] reported that while a small number of BMMSCs were actively engaged in proliferation (approximately 10% at S + G2 + M), the vast majority of cells were in the quiescent state (G0). However, in the study of Nicolin et al. [2007], flow cytometric analysis revealed that PEMF treatment of chondrocytes led to significantly increased cell numbers in the S + G2 + M cell cycle phase. Our findings also showed that PEMF stimulation led to a higher percentage of BMMSCs in the G2/M phase between the 6th and 12th hours, and a higher percentage of BMMSCs in the G0/G1 phase between the 18th and 24th hours in comparison with the control group (Fig. 4B). The results manifested that the first PEMF exposure significantly affected the cell cycle and resulted in more newly divided cells.

The change of cell cycle progression of BMMSCs under PEMF treatment might be attributed to the alteration of cell membrane potential resulting from PEMF exposure. Previously, Panagopoulos et al. [2002] suggested that the possible mechanism of electromagnetic fields on cells is the forced-vibration of all the free ions on the surface of a cell's plasma membrane. Recently, Garner et al. [2007] reported that the

TABLE 2. The Effect of PEMF Treatment on the Surface Markers of BMMSCs Analyzed by Flow Cytometry

Surface marker category	Control	PEMF treatment	
		After 3 days	After 8 days
CD13	+	+	+
CD14	−	−	−
CD29	+	+	+
CD34	−	−	−
CD44	+	+	+
CD45	−	−	−
CD73	+	+	+
CD90	+/−	+/−	+/−
CD105	+	+	+
HLA-ABC	+	+	+
HLA-DR	−	−	−
SH2	+	+	+
SH3	+	+	+
SH4	+	+	+

+, most cells positive; +/−, some cells positive; −, negative.

cytoplasm and nucleoplasm conductivities of Jurkat cells decreased dramatically following nanosecond duration pulsed electric fields. Moreover, Deng et al. [2007] demonstrated that voltage-gated delayed rectifier K^+ current and Ca^{2+}-activated K^+ current channels were changed during progress from G_1 to S phase, and functional expression of ion channels could regulate proliferation in undifferentiated rat mesenchymal stem cells. These findings led us to infer that PEMF exposure changed the expression of ion channels and induced membrane hyperpolarization of BMMSCs and therefore resulted in the alteration of the cell cycle progression.

Although the surface phenotype (Table 2), morphology and multi-lineage differentiation potential of the BMMSCs were not significantly changed by the PEMF (Fig. 4), growth kinetic data and the cell cycle analysis indicated an enhanced growth rate after the first PEMF treatment. In addition, the cell densities achieved by PEMF were significantly higher than those achieved in non-treated conditions. This phenomenon of accelerated growth of BMMSCs due to PEMF may provide more osteoblast progenitor cells, thereby contributing to the healing of bone fractures. This finding facilitates the understanding of the interaction of PEMFs with BMMSC and may partly explain the mechanism underlying the effect of PEMF on bone healing.

ACKNOWLEDGMENTS

We thank Dr. Bruce Simon of EBI for generously providing us the PEMF device for this study.

REFERENCES

Bassett CA, Pawluk RJ, Pilla AA. 1974. Augmentation of bone repair by inductively coupled electromagnetic fields. Science 184:575–577.

Beresford JN. 1989. Osteogenic stem cells and the stromal system of bone and marrow. Clin Orthop Relat Res 240:270–280.

Bianchi G, Banfi A, Mastrogiacomo M, Notaro R, Luzzatto L, Cancedda R, Quarto R. 2003. Ex vivo enrichment of mesenchymal cell progenitors by fibroblast growth factor 2. Exp Cell Res 287:98–105.

Brighton CT, Hozack WJ, Brager MD, Windsor RE, Pollack SR, Vreslovic EJ, Kotwick JE. 1985a. Fracture healing in the rabbit fibula when subjected to various capacitively coupled electrical fields. J Orthop Res 3:331–340.

Brighton CT, Katz MJ, Goll SR, Nichols CE III, Pollack SR. 1985b. Prevention and treatment of sciatic denervation disuse osteoporosis in the rat tibia with capacitively coupled electrical stimulation. Bone 6:87–97.

Brighton CT, Tadduni GT, Pollack SR. 1985c. Treatment of sciatic denervation disuse osteoporosis in the rat tibia with capacitively coupled electrical stimulation. Dose response and duty cycle. J Bone Joint Surg Am 67:1022–1028.

Chang K, Chang WHS, Yu YH, Shih C. 2004a. Pulsed electromagnetic field stimulation of bone marrow cells derived from ovariectomized rats affects osteoclast formation and local factor production. Bioelectromagnetics 25:134–141.

Chang WH, Chen LT, Sun JS, Lin FH. 2004b. Effect of pulse-burst electromagnetic field stimulation on osteoblast cell activities. Bioelectromagnetics 25:457–465.

Chang K, Chang WHS, Huang S, Huang S, Shih C. 2005. Pulsed electromagnetic fields stimulation affects osteoclast formation by modulation of osteoprotegerin, RANK ligand and macrophage colony-stimulating factor. J Orthop Res 23: 1308–1314.

Chang K, Chang WHS, Tsai MT, Shih C. 2006. Pulsed electromagnetic fields accelerate apoptotic rate in osteoclasts. Connect Tissue Res 47:222–228.

Civin CI, Strauss LC, Brovall C, Fackler MJ, Schwartz JF, Shaper JH. 1984. Antigenic analysis of hematopoiesis. III. A hematopoietic progenitor cell surface antigen defined by a monoclonal antibody raised against KG-1a cells. J Immunol 133:157–165.

Conget PA, Minguell JJ. 1999. Phenotypical and functional properties of human bone marrow mesenchymal progenitor cells. J Cell Physiol 181:67–73.

de Haas WG, Watson J, Morrison DM. 1980. Non-invasive treatment of ununited fractures of the tibia using electrical stimulation. J Bone Joint Surg Br 62-B:465–470.

Deng XL, Lau CP, Lai K, Cheung KF, Lau GK, Li GR. 2007. Cell cycle-dependent expression of potassium channels and cell proliferation in rat mesenchymal stem cells from bone marrow. Cell Prolif 40:656–670.

Diniz P, Shomura K, Soejima K, Ito G. 2002. Effects of pulsed electromagnetic field (PEMF) stimulation on bone tissue like formation are dependent on the maturation stages of the osteoblasts. Bioelectromagnetics 23:398–405.

Friedenberg ZB, Brighton CT. 1966. Bioelectric potentials in bone. J Bone Joint Surg Am 48:915–923.

Garner AL, Chen G, Chen N, Sridhara V, Kolb JF, Swanson RJ, Beebe SJ, Joshi RP, Schoenbach KH. 2007. Ultrashort electric pulse induced changes in cellular dielectric properties. Biochem Biophys Res Commun 362:139–144.

Goshima J, Goldberg VM, Caplan AI. 1991. The osteogenic potential of culture-expanded rat marrow mesenchymal cells assayed in vivo in calcium phosphate ceramic blocks. Clin Orthop Relat Res 298–311.

Grace KL, Revell WJ, Brookes M. 1998. The effects of pulsed electromagnetism on fresh fracture healing: Osteochondral repair in the rat femoral groove. Orthopedics 21:297–302.

Guerkov HH, Lohmann CH, Liu Y, Dean DD, Simon BJ, Heckman JD, Schwartz Z, Boyan BD. 2001. Pulsed electromagnetic fields increase growth factor release by nonunion cells. Clin Orthop Relat Res 384:265–279.

Gundle R, Joyner CJ, Triffitt JT. 1995. Human bone tissue formation in diffusion chamber culture in vivo by bone-derived cells and marrow stromal fibroblastic cells. Bone 16:597–601.

Halleux C, Sottile V, Gasser JA, Seuwen K. 2001. Multi-lineage potential of human mesenchymal stem cells following clonal expansion. J Musculoskelet Neuronal Interact 2:71–76.

Heckman JD, Ingram AJ, Loyd RD, Luck JV, Jr., Mayer PW. 1981. Nonunion treatment with pulsed electromagnetic fields. Clin Orthop Relat Res 161:58–66.

Korbling M, Estrov Z. 2003. Adult stem cells for tissue repair - a new therapeutic concept? N Engl J Med 349:570–582.

Lee KD, Kuo TK, Whang-Peng J, Chung YF, Lin CT, Chou SH, Chen JR, Chen YP, Lee OK. 2004. In vitro hepatic differentiation of human mesenchymal stem cells. Hepatology 40:1275–1284.

Lohmann CH, Schwartz Z, Liu Y, Guerkov H, Dean DD, Simon B, Boyan BD. 2000. Pulsed electromagnetic field stimulation of MG63 osteoblast-like cells affects differentiation and local factor production. J Orthop Res 18:637–646.

Lohmann CH, Schwartz Z, Liu Y, Li Z, Simon BJ, Sylvia VL, Dean DD, Bonewald LF, Donahue HJ, Boyan BD. 2003. Pulsed electromagnetic fields affect phenotype and connexin 43 protein expression in MLO-Y4 osteocyte-like cells and ROS 17/2.8 osteoblast-like cells. J Orthop Res 21:326–334.

Luben RA. 1991. Effects of low-energy electromagnetic fields (pulsed and DC) on membrane signal transduction processes in biological systems. Health Phys 61:15–28.

Martin I, Muraglia A, Campanile G, Cancedda R, Quarto R. 1997. Fibroblast growth factor-2 supports ex vivo expansion and maintenance of osteogenic precursors from human bone marrow. Endocrinology 138:4456–4462.

McLeod KJ, Rubin CT. 1992. The effect of low-frequency electrical fields on osteogenesis. J Bone Joint Surg Am 74:920–929.

McLeod KJ, Donahue HJ, Levin PE, Fontaine MA, Rubin CT. 1993. Electric fields modulate bone cell function in a density-dependent manner. J Bone Miner Res 8:977–984.

Minguell JJ, Erices A, Conget P. 2001. Mesenchymal stem cells. Exp Biol Med (Maywood) 226:507–520.

Nicolin V, Ponti C, Baldini G, Gibellini D, Bortul R, Zweyer M, Martinelli B, Narducci P. 2007. In vitro exposure of human chondrocytes to pulsed electromagnetic fields. Eur J Histochem 51:203–212.

Norton LA. 1982. Effects of a pulsed electromagnetic field on a mixed chondroblastic tissue culture. Clin Orthop Relat Res 167:280–290.

Norton LA, Witt DW, Rovetti LA. 1988. Pulsed electromagnetic fields alter phenotypic expression in chondroblasts in tissue culture. J Orthop Res 6:685–689.

Owen M, Friedenstein AJ. 1988. Stromal stem cells: Marrow-derived osteogenic precursors. Ciba Found Symp 136:42–60.

Panagopoulos DJ, Karabarbounis A, Margaritis LH. 2002. Mechanism for action of electromagnetic fields on cells. Biochem Biophys Res Commun 298:95–102.

Pittenger MF, Mackay AM, Beck SC, Jaiswal RK, Douglas R, Mosca JD, Moorman MA, Simonetti DW, Craig S, Marshak DR. 1999. Multilineage potential of adult human mesenchymal stem cells. Science 284:143–147.

Ponte AL, Marais E, Gallay N, Langonne A, Delorme B, Herault O, Charbord P, Domenech J. 2007. The in vitro migration capacity of human bone marrow mesenchymal stem cells: Comparison of chemokine and growth factor chemotactic activities. Stem Cells 25:1737–1745.

Quarto R, Thomas D, Liang CT. 1995. Bone progenitor cell deficits and the age-associated decline in bone repair capacity. Calcif Tissue Int 56:123–129.

Rochefort GY, Delorme B, Lopez A, Herault O, Bonnet P, Charbord P, Eder V, Domenech J. 2006. Multipotential mesenchymal stem cells are mobilized into peripheral blood by hypoxia. Stem Cells 24:2202–2208.

Sakai Y, Patterson TE, Ibiwoye MO, Midura RJ, Zborowski M, Grabiner MD, Wolfman A. 2006. Exposure of mouse preosteoblasts to pulsed electromagnetic fields reduces the amount of mature, type I collagen in the extracellular matrix. J Orthop Res 24:242–253.

Selvamurugan N, Kwok S, Vasilov A, Jefcoat SC, Partridge NC. 2007. Effects of BMP-2 and pulsed electromagnetic field (PEMF) on rat primary osteoblastic cell proliferation and gene expression. J Orthop Res 25:1213–1220.

Sollazzo V, Traina GC, DeMattei M, Pellati A, Pezzetti F, Caruso A. 1997. Responses of human MG-63 osteosarcoma cell line and human osteoblast-like cells to pulsed electromagnetic fields. Bioelectromagnetics 18:541–547.

Sottile V, Halleux C, Bassilana F, Keller H, Seuwen K. 2002. Stem cell characteristics of human trabecular bone-derived cells. Bone 30:699–704.